*Proc. Natl. Acad. Sci. USA*
Vol. 88, pp. 9382–9386, November 1991
Biophysics

# Noninvasive detection of changes in membrane potential in cultured neurons by light scattering

(*Aplysia californica*/cable properties/cell membranes/dark-field microscopy/nonlinear optics)

R. A. STEPNOSKI, A. LAPORTA, F. RACCUIA-BEHLING, G. E. BLONDER, R. E. SLUSHER, AND D. KLEINFELD*

AT&T Bell Laboratories, Murray Hill, NJ 07974

*Communicated by Frank H. Stillinger, July 15, 1991 (received for review March 28, 1991)*

**ABSTRACT** **We report a procedure to detect electrical activity in cultured neurons by changes in their intrinsic optical properties. Using dark-field microscopy to detect scattered light, we observe an optical signal that is linearly proportional to the change in the membrane potential. Action potentials can be recorded without signal averaging. We use the dark-field method to show that there are substantial time delays between activity in the soma and in fine distal processes of identified *Aplysia* neurons. The biophysical basis for the change in optical properties of the neuron was deduced from measurements of the angular distribution of scattered laser light. An analysis of the data indicates that the radial component of the index of refraction of the membrane increases and the tangential components decrease concomitant with an increase in membrane potential. This is suggestive of a rapid reorientation of dipoles in the membrane during an action potential.**

The processing of information by neurons is mediated by their electrical activity. The changes in transmembrane electric fields that accompany this activity are relatively large, on the order of $10^5$ V/cm for action potentials, a value near the dielectric breakdown field for the membrane. It is plausible that these transmembrane fields may noticeably affect the intrinsic optical properties of the membrane and thus provide a means to noninvasively probe the electrical activity of neurons. This possibility was first considered more than 40 years ago by Hill and Keynes (1) and Hill (2), who observed changes in the intensity of light scattered at large angles from nerve during electrical activity. Cohen *et al.* (3) identified additional optical signals in both nerve and giant axons and characterized the dependence of these signals on membrane currents and voltages (4, 5). These intrinsic signals are, unfortunately, relatively small compared to practical limits of detection and thus difficult to observe without extensive signal averaging. As the biophysical mechanism responsible for the voltage-dependent signals is unknown, it is difficult to assess improved schemes for their detection.

Here we reexamine the coupling between the optical properties of neurons and changes in their transmembrane potential. We are motivated by the desire to elucidate a biophysical mechanism that mediates this coupling and by the need to establish a noninvasive means to probe the electrical activity of neurons. Our model system consisted of identified invertebrate neurons. These cells play an increasing role in the study of synaptic plasticity and in the study of emergent properties of small networks. In the present context, they allow us to probe optical changes in a variety of cell types, old versus new outgrowth, and thick versus fine processes.

## EXPERIMENTAL METHODS

**Cell Culture and Electrophysiology.** Juvenile *Aplysia californica* (2–10 g; stage 12), raised in mariculture (18), were purchased from the University of Miami (Florida). Identified neurons in the abdominal and cerebral ganglia were located, microdissected from the ganglion, and maintained in cell culture, as described (6, 7). The cells consist of a soma and one or two axonal stumps at the time of isolation (Fig. 1*A*). They generate an extensive array of processes after 2–3 days *in vitro* (Fig. 1*B*). We estimated the area of cell membrane in the processes as described (8). Standard current-clamp and voltage-clamp methods were used for intracellular stimulation and recording.

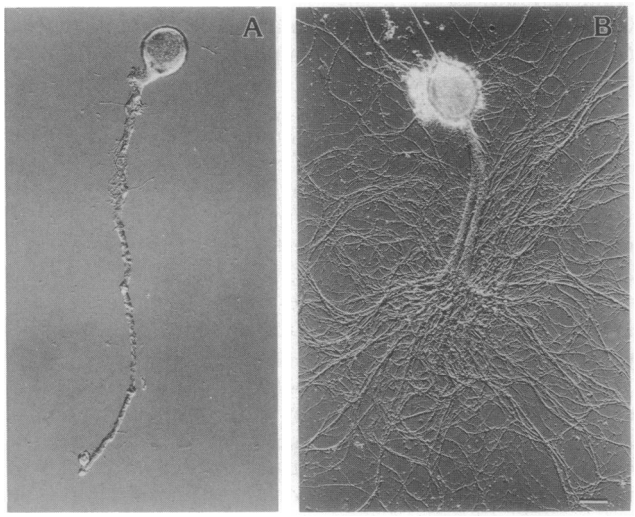


FIG. 1. Photomicrographs of neurons from *Aplysia*. (*A*) A left-upper-quadrant neuron after 0.5 day *in vitro*. (*B*) A left-upper-quadrant neuron after 3 days *in vitro*.

**Dark-Field Microscopy.** The optical system was centered around an upright microscope (UEM; Zeiss) with a ×40 (0.75 n.a.) water-immersion lens (no. 46-17-02; Zeiss) and a (0.80–0.95 n.a.) dark-field illuminator (no. 46-55-05; Zeiss) (see Fig. 2*A Inset*). The cells were plated on a glass coverslip that formed the bottom of a 50-mm Petri dish with a hole drilled in the bottom. For all records shown, except those in Fig. 4*B*, the light source was a 100-W quartz tungsten lamp (Xenophot HLX; Osram, Berlin) that was filtered by 1 cm of heat-absorbing glass. The maximum power at the preparation was $1 \times 10^{-3}$ W and the relative fluctuations (peak to peak) in the intensity were typically $\gtrsim 3 \times 10^{-5}$ in the frequency range 1–300 Hz. For measurements of the wavelength dependence of the optical changes, the heat-absorbing glass was replaced by interference filters spanning the range 0.40–0.70 μm with a half-width at half-maximal transmission of 0.03 μm (no. 57800; Oriel, Stamford, CT). For the records shown in Fig. 4*B*, the light source was a hexagonal array of 13 light-emitting

The publication costs of this article were defrayed in part by page charge payment. This article must therefore be hereby marked "*advertisement*" in accordance with 18 U.S.C. §1734 solely to indicate this fact.

*To whom reprint requests should be addressed at: Room 1C-463, AT&T Bell Laboratories, 600 Mountain Avenue, Murray Hill, NJ 07974.

diodes that emit at 0.66 μm (no. 130CRP; AND, Burlingame, CA). The maximum power at the preparation was $1 \times 10^{-5}$ W, but the fluctuations were shot-noise-limited for frequencies down to 1 Hz. The scattered light was collected from a field with a radius of 50–90 μm and focused with a ×10 eyepiece in an auxiliary port of the microscope onto a photodiode (no. UV100BG; EG & G, Holliston, MA) with a conversion gain of 0.3 A/W.

**Angular Resolved Scattering.** A laser light scattering apparatus was constructed on a vertically held optical table (see Fig. 3*A Inset*). The Petri dish that contained the neurons and a pair of micromanipulators for use in electrophysiological measurements was supported by an *x–y* translation stage mounted directly to the table. A 1-mW HeNe laser (0.63 μm) (no. 1508; Uniphase, San Jose, CA) was spatially filtered and focused onto the preparation with a lens (focal length $f = 15$ cm). The beam was unpolarized and measured to have a Gaussian intensity profile with a radius ($1/e^2$) of 70 μm at the focus. It propagated along an axis, $\hat{x}$, that was perpendicular to the axis centered along the axon of the cell, $\hat{z}$ (see Fig. 3*A Inset*). The scattered light was detected with a photodiode that was mounted on a rotary stage whose axis of rotation coincided with $\hat{z}$. The detector could be positioned with an accuracy of 0.1° and had an acceptance angle of 0.2°.

## RESULTS

**Basic Response.** Our initial experiments were directed toward determining if electrical activity could substantially modulate the optical properties of isolated neurons. In principle, any change in the index of refraction of the cytoplasm or membrane of the neuron will change the way it scatters light. We searched for such effects using a microscope equipped with a dark-field illuminator (Fig. 2*A Inset*). In this scheme, the preparation was irradiated at an oblique angle and about half of the light that was scattered beyond a minimum angle, $\theta_0 \approx 3°$, was collected with an objective.

We observed that the intensity of the scattered light $S$ was modulated by changes in the membrane potential. The functional relationship between the change in intensity $\Delta S$ and the membrane potential was established in two ways. (*i*) The optical change from a small field that contained a segment of the axon of a newly isolated cell (Fig. 1*A*) was compared with the change measured with an intracellular electrode that was located just outside the optical field (Fig. 2*A Inset*). The optical signal tracked the electrically measured action potential that was elicited by the injection of a positive current pulse (Fig. 2*A*). A correspondence between the optical and electrical signals was similarly observed when the cell was hyperpolarized by injecting negative current pulses (data not shown). (*ii*) In another approach, we measured the optical changes from neurons that were voltage-clamped and stepped to potentials both above and below their resting potential. The fractional change in intensity $\Delta S/S$ depended linearly on the change in membrane potential, $\Delta V = V - V_{rest}$, over a range of nearly 200 mV that was inclusive of physiological potentials. Although the linearity of the change was quite good for each neuron (Fig. 2*B*), the proportionality constant varied among different cells and fields of view for the same cell. We found $(\Delta S/S)/\Delta V = 8 \pm 5 \times 10^{-6}$ mV$^{-1}$ (mean ± SD) for a set of 20 cells; the uncertainty (SD) refers to the standard deviation for measurements on different cells. The value of the constant was essentially independent of wavelength over the visible spectrum of light (data not shown). Note that no signal was observed from the soma (see Fig. 4*D*), apparently as a consequence of the large background intensity caused by scattering from granular and pigmented organelles.

The optical changes observed from fine processes with the dark-field scheme were sufficiently large to be observed without signal averaging. When neurons were injected with a pulse of positive current $\Delta I$, subthreshold depolarization and spike trains were clearly seen from a field with multiple fine processes (Fig. 2*C*). The signal/noise (peak-to-peak) ratio for

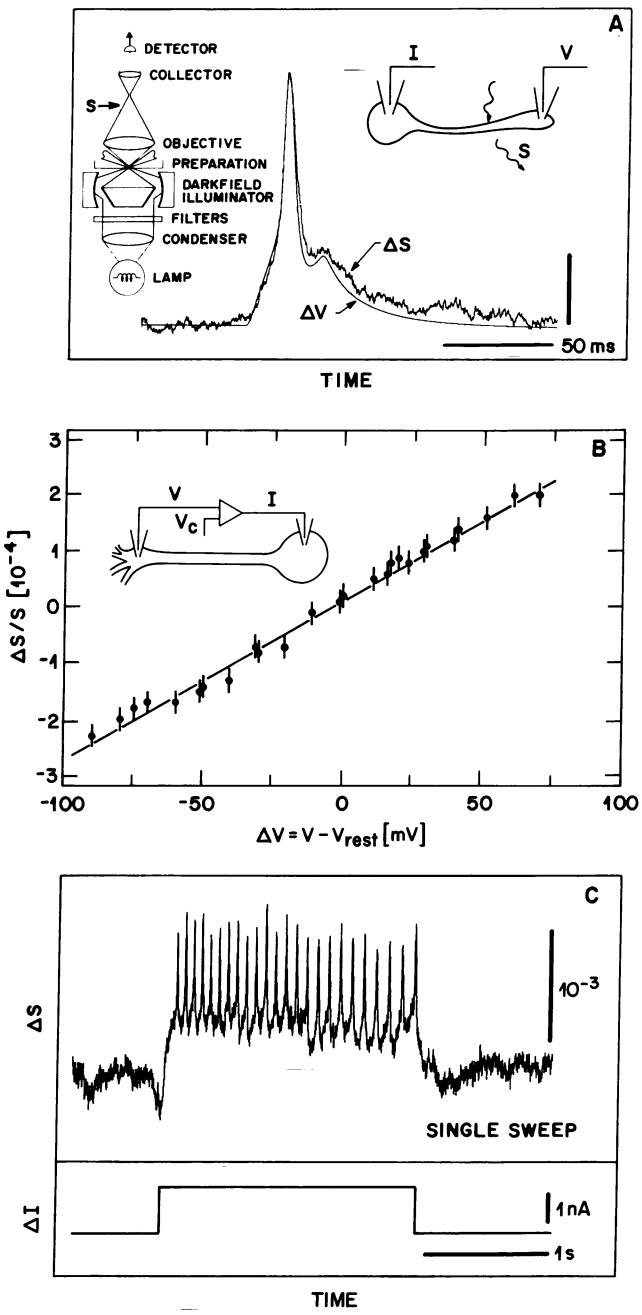


FIG. 2. Measurement of electrical activity by the detection of scattered light in a microscope equipped for dark-field illumination. (*A*) Simultaneous optical and intracellular records from the axonal stump of a neuron after 0.5 day *in vitro* (Fig. 1*A*). The area of membrane in the field was $1 \times 10^4$ μm$^2$ and consisted almost exclusively of old outgrowth. Data are the average of 500 traces; $S = 42$ nA. (*Inset*) Schematic diagram of the apparatus. (*B*) Demonstration of the linear relationship between the change in the intensity of scattered light and the change in transmembrane potential. The neuron was voltage-clamped and the potential was stepped from a holding value of $V_{rest} = -50$ mV to the desired value $V$ with 300-ms pulses repeated every 1100 ms. Data points are the average of 200 traces; $S = 1.9$ nA. (*C*) Real-time optical record of a train of spikes in a left-upper-quadrant cell after 3 days *in vitro* (e.g., Fig. 1*B*). The train was induced by a current pulse, $\Delta I$. The optical changes were measured from a field that included the distal end of the axonal stump and many fine processes. The cell was slightly hyperpolarized before the pulse to accentuate the initial subthreshold depolarization. The amplitude of the spikes appears uneven as a consequence of sampling. The area of membrane in the field was $1 \times 10^4$ μm$^2$ and consisted of both new and old outgrowth. $S = 140$ nA.

detecting a spike was 5–10 and was limited by random motion of precipitates from the growth medium that adhered to the processes. In principle, the signal/noise ratio could be substantially greater if the dominant noise source was thermal fluctuations of the lamp or shot noise. Lastly, we recorded continuously for periods of up to 10 hr with no discernible change in the magnitude or the shape of the action potential.

**Biophysical Mechanism for the Optical Changes.** The above results establish that there is a linear coupling of the optical properties of a neuron with its membrane potential. This coupling, in general, will depend on both the spatial profile of the index of refraction of the neuron $n(r)$ and changes in this profile $\Delta n(r)$ during activity. We quantified the index profile through a series of laser light scattering experiments. The intensity of light that was scattered transverse to the orientation of an axon $S(\theta)$ was measured as a function of the azimuthal angle $\theta$ for axons of known radii $R$ (Fig. 3*A Inset*).

The dominant part of the scattered light was independent of activity (Fig. 3*A*). The intensity was sharply peaked near $\theta = 0°$ and fell off as a series of peaks and troughs, with exponentially decreasing amplitude, as the scattering angle increased. Further, the scattering patterns often were asymmetric. The spatial profile of the index was derived from a comparison of the observed patterns from 42 cells ($4\ \mu m \leq R \leq 10\ \mu m$) with those calculated for scattering from dielectric cylinders. The spatially averaged value of the index $\langle n \rangle$ depends only on the relative intensity of the zeroth scattering peak (Fig. 3*A*, *). We found $\langle n \rangle = 1.016 \pm 0.005$ (mean ± SD) relative to the index of saline. The radial variation of the index affected the rate at which the intensity falls off with increasing angle. Qualitatively, the observed fall off was greater than that expected for scattering from a uniform dielectric cylinder (9) (Fig. 3*A*, dotted curve). It can be explained by an index that is higher near the center of the axon than near the outer membrane. For convenience in estimating the spatial variation, we parameterized this spatial variation in terms of a Gaussian profile for the radial dependence of an isotropic index, i.e.,

$$n(r) = 1 + [n(r_0) - 1]e^{-(r-r_0)^2/2\sigma^2} \quad \text{with } r < R, \quad [1]$$

where $n(r_0)$ is the maximum value of the index, $r_0$ is the offset of the maximum relative to the center of the axon, $\sigma$ is the width of the profile, and $R$ is the measured radius of the axon. These parameters satisfy the relationship $\langle n(r) \rangle = \langle n \rangle$. The scattering pattern calculated for this profile (*Appendix*) (Fig. 3*A*, solid curve) agreed well with the observed pattern in >70% of the cells. We found $n(r_0) = 1.021 \pm 0.005$ (mean ± SD), $r_0/R = 0.3 \pm 0.3$, and $\sigma/R = 1.0 \pm 0.3$.

These results showed that the maximum value of the index occurred close to, but not necessarily at, the center of an axon and that the incremental value of the index near the membrane was ≈40% lower than that near the center. Further, the addition of a membrane to the cylinder with index and thickness appropriate for a neuron (10) did not substantially affect the calculated scattering pattern. Thus the static optical properties of the cell were dominated by the index of the cytoplasm and not of the membrane.

We next considered the change in scattered light $\Delta S(\theta)$ that occurred concomitantly with a voltage spike (Fig. 3*B Inset*). This change was superimposed on the dominant scattering $S(\theta)$. The measurements of $\Delta S(\theta)$ involved extensive averaging because of the large fluctuations in the intensity of laser light. We observed that $\Delta S(\theta)$ alternates in sign as a function of the scattering angle (Fig. 3*B*). The sign and magnitude of the change at small angles, which constitute the dominant contribution to the integral of the change in scattered light, are in agreement with those observed in the measurements of the integrated scattered light with dark-field illumination.

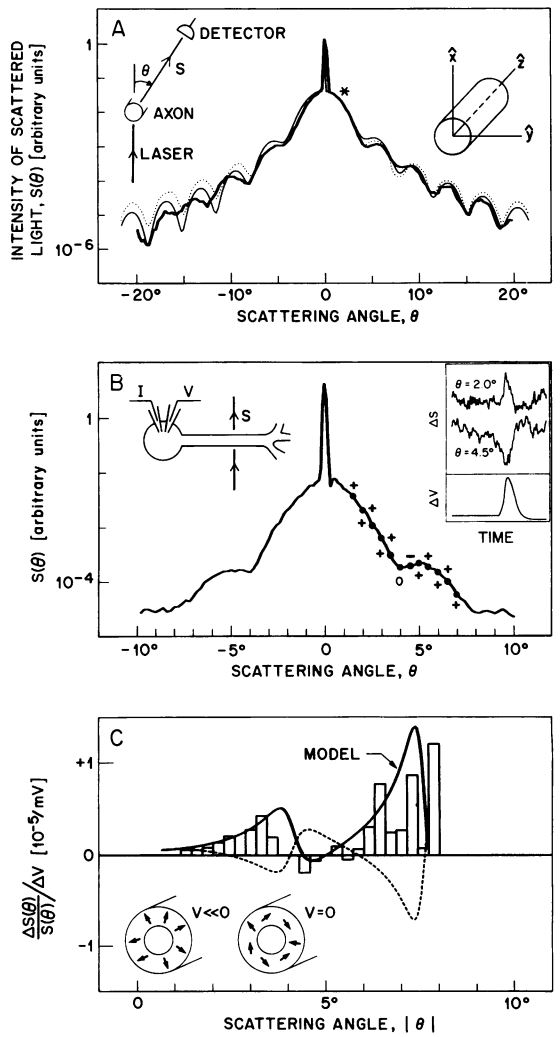


FIG. 3. Optical properties of neurons derived from laser light scattering measurements. (*A*) Intensity of scattered light $S(\theta)$ measured as a function of the scattering angle $\theta$ (*Left inset*) for an axon ($R = 5.8\ \mu m$) after 2 days *in vitro*. The dotted curve overlying the data (thick line) represents the pattern calculated for scattering by a uniform dielectric cylinder (*Right inset*) with $\langle n \rangle = 1.025$. The thin solid curve represents the pattern calculated for scattering by a dielectric cylinder with a Gaussian index profile (Eq. 1) with $n(y_0) = 1.031$, $y_0 = r_0/2 = 0.5\ \mu m$, and $\sigma = 7.3\ \mu m$. (*B*) Static scattering pattern of a neuron ($R = 5.0\ \mu m$) for which the change in intensity $\Delta S$ was measured at select angles as a function of electrical activity. +, Angles at which an increase in intensity was observed concomitant with a spike; −, angle at which a decrease was observed; ○, angle at which no change was discernible. (*Right inset*) Change in intensity at two angles in response to the injection of a pulse of current. The intracellular record of the spike is shown below. Data points are the average of 200 traces; $S = 140\ \mu A$. (*C*) Fractional change in intensity as a function of angle. Bars represent data from seven neurons (85 individual values), with radii between 4 μm and 6 μm that were normalized to a radius of 5.0 μm and binned at 0.5° intervals. The fractional standard deviation is ≈20% for data at small angles and ≈100% at the largest angles. The solid curve is a fit of the anisotropic model (Eq. 2) to the data with a static index (Eq. 1) parameterized by $n(0) = 1.018$, $\sigma = 7.1\ \mu m$, and $R = 5.0\ \mu m$. (*Inset*) Cartoon of the change in alignment of dipoles in the membrane that is hypothesized, within the context of the model, to occur in response to an increase in potential. The dashed curve is a fit of an isotropic model to the data for which the strength of the dipoles changes while their alignment remains fixed (see text).

The observed angular dependence of $\Delta S(\theta)/S(\theta)$ could be understood in terms of a model of dipoles in the membrane that preferentially orient along the direction of the transmem-

brane electric field (Fig. 3*C Inset*). The membrane could have one index, $n_r$, for light whose polarization is normal to the membrane and different equivalent indices, $n_\theta = n_z$, for light whose polarization is tangent to the membrane. For a small change in the average alignment of the dipoles, the indices change according to

$$\Delta n_r = -2\Delta n_\theta = -2\Delta n_z \equiv n^{(1)} \frac{\Delta V}{d} \quad \text{with } r = R, \quad [2]$$

where $n^{(1)}$ is the nonlinear index and $d$ is the thickness of the membrane. A positive value of $n^{(1)}$ corresponds to a greater alignment of dipoles at the resting potential than near the peak of an action potential (Fig. 3*C Inset*). We calculated (*Appendix*) the expected angular dependence of $\Delta S(\theta)/S(\theta)$ (Eq. 2 with the static index profile of Eq. 1). The predicted alternation between positive and negative changes as a function of the scattering angle was in good agreement with the data (Fig. 3*C*, solid curve). The form of this alternation was independent of the magnitude of $n^{(1)}$. We estimated that $n^{(1)} = 1.2 \pm 0.4 \times 10^{-8}$ $cmV^{-1}$ (mean ± SD), which corresponds to an average phase retardation of light by $(\pi/2) \times 10^{-4}$ radians during a spike. A predicted decrease in the intensity at $\theta = 0°$ was also in agreement with our observations (data not shown).

As a means of probing the uniqueness of the model (Eq. 2) for the observed optical changes (Fig. 3 *B* and *C*), we considered the angular dependence of $\Delta S(\theta)/S(\theta)$ predicted for alternate models. One possibility is an isotropic change in the indices of the membrane; i.e., $\Delta n_r = \Delta n_\theta = \Delta n_z \propto \Delta V$. Such a change could arise, for example, if the thickness of the membrane was modulated by the membrane voltage. The predicted angular dependence of $\Delta S(\theta)/S(\theta)$ for this model undergoes a reversal in sign within the zeroth scattering peak, in marked contrast to the experimental evidence (Fig. 3*C*, dashed curve). A second possibility is that only the radial index is modulated by changes in the membrane potential; i.e., $\Delta n_r \propto \Delta V$ and $\Delta n_\theta = \Delta n_z = 0$. The predicted angular dependence of $\Delta S(\theta)/S(\theta)$ for this model also exhibited a reversal in sign within the zeroth scattering peak and was incompatible with the data (Fig. 3 *B* and *C*). Lastly, although the time course (Fig. 2*A*) and linearity (Fig. 2 *A* and *B*) of the optical signals implied that the change in optical properties was confined to the membrane, we considered the possibility of a voltage-dependent change in the average index of the cytoplasm $\langle n(r) \rangle$ (Eq. 1). For this model, the sign of $\Delta S(\theta)/S(\theta)$ was predicted to remain the same at all angles, again in marked contrast with the data (Fig. 3 *B* and *C*). We conclude that predictions based on the model of dipole reorientation in response to changes in the transmembrane potential (Eq. 2) are uniquely consistent with the experimental evidence whereas predictions based on other simple models are inconsistent with the evidence (Fig. 3*C*).

**Propagation of Activity in Fine Processes.** The dark-field method provides a means to record the electrical activity in cultured cells that is complementary to optical methods that rely on the use of potentiometric dyes (11–14). An analysis based on the characterization of the optical index (Eqs. 1 and 2) showed that the fractional change in intensity of the scattered light should scale as the ratio of the membrane area to the volume of the cell; i.e., $\Delta S/S \propto 1/R$. By comparison, the fractional change in the intensity of transmitted light scales linearly with the radius for methods that use bright-field illumination to probe dyes and the fractional change in the intensity of emitted light is independent of the radius for methods that utilize fluorescence. The signal/noise ratio for any of these methods is linearly related to the fractional change in the intensity of light when, as in the present case, the dominant noise source is movement of the preparation or thermal fluctuations in the lamp. Although the form of this relation is somewhat different with other noise sources, we conclude that light scattering is ideal for observing signals from fine processes, whereas other methods are best for larger structures.

We used the dark-field technique in two paradigms to assess if the fine processes of cultured neurons were isopotential with their parent soma. First, we chose cells with profuse new growth and compared the optically recorded action potential

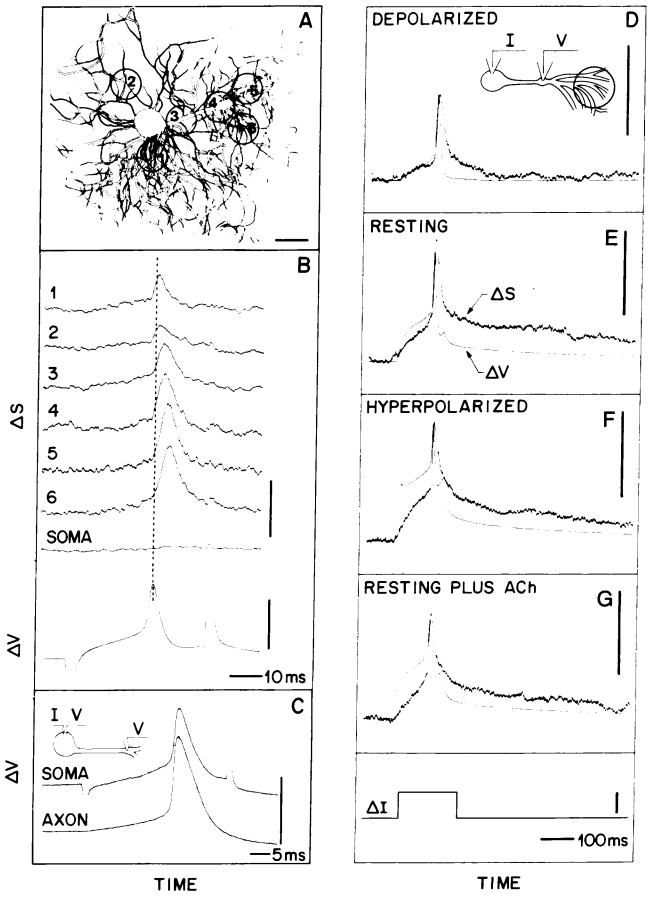


FIG. 4. Optically detected electrical activity from the axonal stump and fine processes of two different left-upper-quadrant neurons by using the dark-field method. (*A–C*) Relation among signals recorded from different parts of one cell. (*D–G*) Relation between the optically recorded activity in the distal process and the electrically recorded signal in the soma of a second cell. (*A*) Sketch of the neuron, examined after 5 days *in vitro*, that was used for the records in *B* and *C*. The circles correspond to different fields (60-μm radius). The areas of membrane were $2 \times 10^4$ μm², $6 \times 10^3$ μm², $1 \times 10^4$ μm², $2 \times 10^4$ μm², $2 \times 10^4$ μm², and $2 \times 10^4$ μm² for fields 1–6, respectively. (*B*) Optical records for activity in different fields along with the concomitant change in intracellular potential. Action potentials were elicited by injecting current through a single electrode placed in the soma. Spikes are seen in fields containing only fine processes (fields 1, 2, 5, and 6) and those containing the axonal stump (fields 3 and 4). The signal from each field is believed to be dominated by contributions from fine processes. No signal is observed from a field encompassing the soma ($\Delta S/S < 5 \times 10^{-6}$). Data are the average of 100–150 traces; $S$ = 10–20 nA. (*C*) Simultaneous intracellular records for the soma and the distal end of the axonal stump. (*D–G*) Optical records from the finest distal process along with the concomitant intracellular signal recorded from the soma. The area of membrane in the field was $1 \times 10^4$ μm². (*D*) The potential at the soma was maintained just below threshold, $V = -35$ mV, by the continuous injection of depolarizing current. (*E*) The potential was $V = -55$ mV with no current injected between pulses. (*F* and *G*) The potential was maintained at $V = -90$ mV by, respectively, the continuous injection of hyperpolarizing current or the addition of 100 μM acetylcholine to the bath. Data are the average of 100 traces; $S$ = 45 nA.

in the processes with the electrically recorded signal in the soma. The peak of the optical signal for fields of view near the soma coincided with the electrical spike in the soma (Fig. 4 *A* and *B*, fields 1–4), whereas the signal in fields away from the soma was delayed and broadened. The delay was greatest for fields containing only fine distal processes (Fig. 4 *A* and *B*, fields 5 and 6) and was negligible between the soma and the thick axonal stump (Fig. 4*C*). The data show that spikes propagate at a speed of ≈10 cm/s in processes with radii of 1–2 μm, consistent with the speed estimated for electronic spread in processes with linear cable properties (15). The broadening of the spike in the optical records is consistent with the dispersion that accompanies electronic spread of activity. In the second paradigm, we compared the rate of subthreshold depolarization observed optically from distal processes with that observed in the soma (Fig. 4*D–G*). With the cell poised just below threshold, the rate of depolarization was low and was essentially the same in the processes as in the soma (Fig. 4*D*). However, with the cell poised at hyperpolarizing potentials, either by the injection of current or the addition of acetylcholine (16), the rate of depolarization in the processes was substantially less than that in the soma (Fig. 4 *F* and *G*). These results demonstrate that the fine processes are electrotonically distant from the soma and suggest that these processes support only the passive spread of electrical activity.

## DISCUSSION

The optical signals we observe in electrically active neurons depend linearly on the transmembrane potential. This result contrasts with those found in early studies of optical changes that accompany electrical activity for which the intensity of the scattered light was found to be proportional to membrane currents (4) or was a nonlinear function of the membrane potential (5). These studies made use of either giant axons, whose radii are up 100 times that of *Aplysia* processes, or nerve. Slow current-dependent signals from giant axons result from a change in the volume of the space between the axon and its sheath that occurs secondary to electrical activity (4). These changes are not expected to be present with cultured neurons. The apparent absence of linear voltage-dependent signals in giant axons (5) may be understood from sensitivity considerations. As shown for the *Aplysia* neurons, the dominant contribution to the voltage-dependent change in scattered light arises from the zeroth peak in the scattering pattern (Fig. 3*B*). The width of the peak scales roughly as $1/R$. Thus it is expected to lie too close to the forward direction for giant axons (≈0.1° for an axon with a 300-μm radius) to be resolved.

Our characterization of the optical index (Eqs. 1 and 2) allows one to assay the feasibility of alternate measurement schemes. One possibility is to detect changes in retardation with a microscope based on a Mach–Zehnder interferometer. This procedure is complimentary to light scattering and, in principle, measurements can be made with a diffraction limited spot. A second possibility is to image the electrical activity with dark-field or interferometric techniques. The measurement of electrical activity in optically thick preparations, such as ganglia and brain, may be problematic. One possibility is to observe activity near the surface of the preparation by changes in the intensity of back-scattered light; i.e., at $\theta = 180°$. A second is to use an interferometric scheme that incorporates phase conjugate optics to compensate for distortions in the optical wavefront that are introduced by the preparation.

## APPENDIX

The intensity of scattered light as a function of the angle relative to the incident beam was calculated numerically for scattering from a dielectric cylinder with radius $R$. The cylinder was taken to lie along $\hat{z}$, and beam was taken to propagate along $\hat{x}$. The electric field of the incident beam was unpolarized and had a Gaussian profile, i.e., $E_y(x = 0^-, y, z) = E_z(x = 0^-, y, z) \propto \exp(-(y^2 + z^2)/2w^2)$, where $w >> R$ is the width at the focus of the beam ($x = 0$). The surface of constant phase lies in the $y$–$z$ plane that passes through the center of the axon. In the limit that the average index of the cylinder is close to 1.00, we can approximate the cylinder as a strip of phase-retarding material in the $y$–$z$ plane whose optical thickness corresponds to the cross section of the cylinder. This limit is satisfied in the present work. The isotropic static retardation is

$$\phi(y) = \frac{2\pi}{\lambda} 2 \int_0^{\sqrt{R^2 - y^2}} dx[n(x, y) - 1],$$

where $n(x, y) = 1 - [n(r_0) - 1]\exp\{-[x^2 + (y - y_0)^2]/2\sigma^2\}$ (Eq. 1 with $y_0 = r_0/2$). The index of the membrane is taken to be isotropic except for the small contributions given by Eq. 2. The activity-dependent retardation is

$$\Delta\phi_y(y) = \frac{2\pi}{\lambda} 2 \int_{\sqrt{(R-d)^2 - y^2}}^{\sqrt{R^2 - y^2}} dx\Delta n_y(x, y),$$

with an analogous expression for $\Delta\phi_z(y)$, where $\Delta n_y(x, y) \simeq \Delta n_r \sin^2\theta + \Delta n_\theta \cos^2\theta$ with $\theta = \tan^{-1}(y/x)$ and $\Delta n_z(x, y) = \Delta n_z$ are the leading terms in the index ellipsoid (17) for the membrane. The electric field just beyond the strip is thus $E_y(0^+, y, z) \propto E_y(0^-, y, z)\exp\{i[\phi(y) + \Delta\phi_y(y)]\}$, with an analogous expression for $E_z(0^+, y, z)$. The scattered intensity is $S(\theta) \propto |E_y(x, y, 0)|^2 + |E_z(x, y, 0)|^2$, where $x^2 + y^2 =$ constant and the values of $E_y(x, y, 0)$ and $E_z(x, y, 0)$ are calculated from $E_y(0^+, y, z)$ and $E_z(0^+, y, z)$, respectively, using Kirchoff's method (17). The change in intensity $\Delta S(\theta)$ is found by calculating $S(\theta)$ for different values of $\Delta V$ (Eq. 2).

We thank B. M. Salzberg and J. A. Valdmanis for stimulating our interest in this problem; J. P. Allen, L. B. Cohen, K. R. Delaney, W. Denk, and A. R. Kay for useful discussions; and R. H. Eick for technical assistance.

1. Hill, D. K. & Keynes, R. D. (1949) *J. Physiol. (London)* **108**, 278–281.
2. Hill, D. K. (1950) *J. Physiol. (London)* **111**, 283–303.
3. Cohen, L. B., Keynes, R. D. & Hille, B. (1968) *Nature (London)* **218**, 438–441.
4. Cohen, L. B., Keynes, R. D. & Landowne, D. (1972) *J. Physiol. (London)* **224**, 727–752.
5. Cohen, L. B., Keynes, R. D. & Landowne, D. (1972) *J. Physiol. (London)* **224**, 701–725.
6. Schacher, S. & Proshansky, E. (1983) *J. Neurosci.* **3**, 2403–2413.
7. Kleinfeld, D., Raccuia-Behling, F. & Chiel, H. J. (1990) *Biophys. J.* **57**, 697–715.
8. Kleinfeld, D., Raccuia-Behling, F. & Blonder, G. E. (1990) *Phys. Rev. Lett.* **65**, 3064.
9. Strutt, W. S. [Lord Rayleigh] (1918) *Philos. Mag.* **36**, 365–376.
10. Huang, C. & Thompson, T. E. (1965) *J. Mol. Biol.* **13**, 183–193.
11. Grinvald, A., Ross, W. N. & Farber, I. C. (1981) *Proc. Natl. Acad. Sci. USA* **78**, 3245–3249.
12. Ross, W. N., Arechiga, H. & Nicholls, J. G. (1987) *J. Neurosci.* **7**, 3877–3887.
13. Parsons, T. D., Salzberg, B. M., Obaid, A. L., Raccuia-Behling, F. & Kleinfeld, D. (1991) *J. Neurophysiol.* **66**, 316–333.
14. Chien, C.-B. & Pine, J. (1991) *Biophys. J.* **60**, 697–711.
15. Jack, J. J. B., Nobel, D. & Tsien, R. W. (1983) *Electric Current Flow in Excitable Cells* (Oxford Univ. Press, London).
16. Camardo, J., Proshansky, E. & Schacher, S. (1983) *J. Neurosci.* **12**, 2614–2620.
17. Born, M. & Wolf, E. (1980) *Principles of Optics* (Pergamon, New York), 6th Ed.
18. Kriegstein, A. R., Castellucci, V. F. & Kandel, E. R. (1974) *Proc. Natl. Acad. Sci. USA* **71**, 3654–3658.